Development of a Control Algorithm for an Active Limited Slip Differential

F. Assadian, M. Hancock and M. C. Best
Cranfield University, Jaguar Cars Ltd., Loughborough University

Cranfield, Bedfordshire, MK43 0AL, United Kingdom
Phone: (+44) 1234 754657
Fax: (+44) 1234 758259
E-mail: f.assadian@cranfield.ac.uk

Mechanical limited slip differentials provide a low cost traction solution. However, their passive nature means that they cannot adapt to different scenarios and their yaw moment generation potential cannot be used for vehicle handling or stability control. Active limited slip differentials are becoming popular as they are able to exploit this potential and also achieve a better traction compromise due to their ability to adapt to different scenarios. This paper describes the development of a control algorithm for an ALSD fitted to a RWD sports saloon vehicle.

Key Phrases: Yaw Control, Powertrain & Drivetrain Control, Energy Efficient Vehicles.

1. INTRODUCTION

Vehicle handing control systems are becoming commonplace in the motor industry. The majority of such systems currently in production are Electronic Stability Control (ESC) systems that use brake interventions at individual wheels to develop yaw moments that protect vehicle stability at times when it would otherwise be compromised. These systems are highly effective from a vehicle dynamics and stability perspective and are now standard fitment on premium vehicles. However, for the next generation of vehicle handling control systems, the focus of the premium vehicle manufacturers is not just to improve stability but also to increase driver enjoyment whilst driving both below and at the limits of adhesion. Brake based systems are not conducive to driver enjoyment because they tend to be highly intrusive, causing sudden decelerations and loss of vehicle speed.

Alternative actuation systems are therefore being considered that may provide increased stability, without the intrusiveness of a brake based system. Active limited slip differentials (ALSDs) that allow electronically controlled transfer of torque between the driven wheels are one such alternative. Controlled torque transfer across an axle allows a yaw moment to be generated that can be used to increase vehicle stability and because wheel torque is reapportioned, rather than reduced, this increase in stability can be achieved in a less intrusive manner than would be possible with a brake based control system.

In order to deliver stability benefits on a real vehicle, a practical ALSD control algorithm is required. Key challenges with respect to the development of such a controller are the semi-active nature of the actuator and its relatively slow dynamic response (in comparison to a brakes system). One of the alternatives for designing a controller which can address these key challenges is the utilization of a H-Infinity control (Hinf), a modern control synthesis that offers the capability to formulate an optimization problem in the frequency domain. This paper describes the development of a practical feedback controller for an ALSD that meets these challenges. The controller is applied to an actual vehicle and the stability control performance of the system is assessed.

2. ACTIVE DIFFERENTIALS

Traditional open differentials distribute the same amount of torque to the left and right wheels, while allowing them to rotate at different speeds. Active differentials utilize clutches to provide a controlled left/right (or front/rear) torque distribution to the wheels, thus resulting in enhancing traction control and yaw stability control performance without being intrusive for the driver (brake activation can be avoided) [1].

The active limited slip differential (**ALSD**; Fig. 1a) utilizes a single clutch that connects the differential rotating case with one of the output shafts. Since the case speed is equal to $\omega_c = (\omega_1 + \omega_2) / 2$ [2] and the clutch always transfers the torque from its faster to slower shaft, the ALSD can provide torque transfer to the slower wheel only. The direction of torque transfer, and therefore the direction of the yaw moment applied is determined by the wheel speed difference across the axle. In this sense an ALSD is a semi-active device. While this is effective for traction control (the slower

wheel has better traction), it is restricted to oversteer compensation only when being used as a yaw stability control device since only understeer torque can be generated (torque transfer to the inner/slower wheel).

Torque vectoring differentials (TVD) can transfer the torque to either the slower or faster wheel, thus providing full active yaw control functionality (understeer and oversteer can be generated). This can be achieved by extending the ALSD hardware by additional gearing and an additional clutch, as shown in Fig. 1b [1]. The spur gear set z_1-z_4-z_5-z_2 speeds up the input shaft of the clutch F_2 (the gear ratio $h_2 = z_1z_5 / (z_4z_2) > 1$), thus allowing the clutch F_2 to transfer the torque to the right wheel even if it rotates faster than the left wheel. Similarly, the gear set z_1-z_4-z_6-z_3 slows down the input shaft of the clutch F_1 ($h_1 = z_1z_6 / (z_4z_3) < 1$), so that the torque can be taken from the right wheel and brought to the left wheel even if the left wheel rotates faster than the right wheel. For the particular values of gear ratios $h_1 = 0.875$ and $h_2 = 1.125$, the torque can be transferred to the faster wheel if its speed is not more than 28.6% larger than the slower wheel [1,3]. This is an ample reserve for a variety of vehicle dynamics control scenarios. Some other characteristic kinematic structures of TVDs are described and analyzed in [4,3].

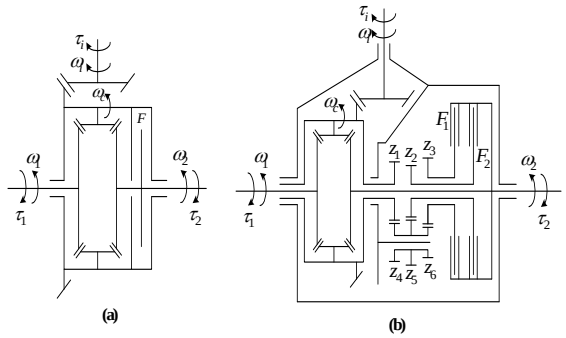

Fig. 1 Kinematic schemes of active limited slip differential (a) and torque vectoring differential (b)

In addition to the disadvantage of constrained torque transfer direction, the ALSD can suffer from an inaccurate and slow torque transfer response [5]. This is because the engaged clutch can easily become locked for mild turns (the slip speed $\omega_f = (\omega_1 - \omega_2) / 2$ drops to zero), and the locked clutch is not controllable. On the other hand, due to the use of additional gearing the TVD's clutches have an increased slip speed and can rarely be locked. This gives favorable controllability, but the power losses are larger than for the ALSD.

The vehicle used for this investigation is a rear wheel drive sports saloon. A schematic of the ALSD employed is shown in Fig. 2. It features a wet friction clutch pack that transfers torque between the two drive shafts. The clamping force on the clutch pack is controlled by an electric motor driven actuation system that acts through a ball and ramp mechanism. The response of the differential can be characterized by a pure delay followed by a first order lag (Fig. 3).

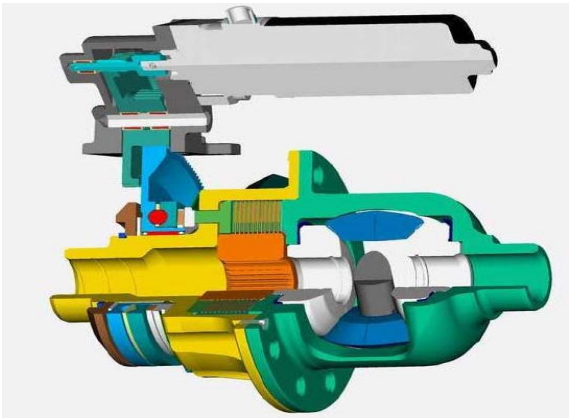

Fig. 2 Schematic of the AL SD fitted to the prototype vehicle

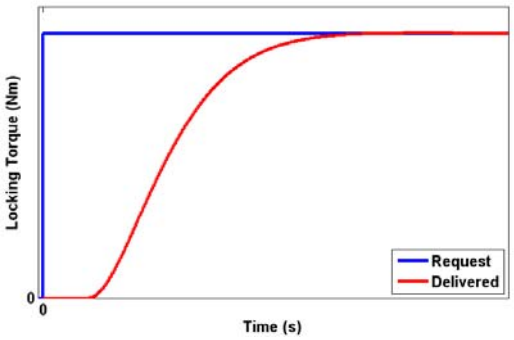

Fig. 3 Actuator Time Response

3. CONTROL DESIGN

It is clear from Section 2 that a controlled differential is capable of influencing performance in the two relatively broad areas of yaw moment / stability and traction [6]. This paper describes only the development of the yaw stability control algorithm; the traction control development will be addressed in future work.

The structure of the ALSD stability controller is shown in Fig. 4. As can be observed from the figure, the control is based on a reference model. This reference is a relatively simple vehicle model that generates a target yaw rate based on vehicle speed, driver steering input and estimated surface friction coefficient. The error between the target yaw rate and the vehicle's actual yaw rate is then fed through a feedback controller in order to generate a required torque transfer for the ALSD. Since the ALSD can only generate an understeer developing yaw moment (when off throttle), this torque transfer is only applied when the calculated yaw error indicates oversteer. It is the design of the feedback controller that will be the focus of this Chapter.

The plant model used to design the controller is a two degree of freedom linear bicycle model. The degrees of freedom are yaw and sideslip velocity.

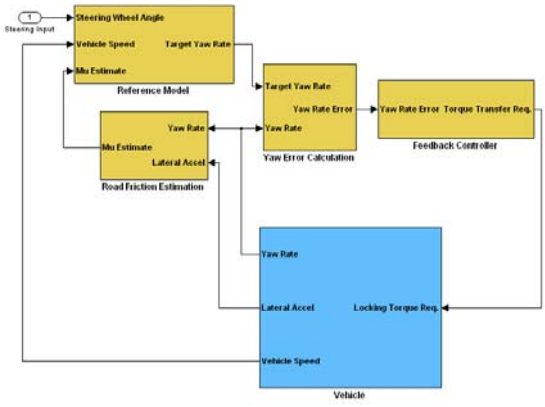

Fig. 4 Controller Structure

In state-space form, this model may be written as,

$$\begin{bmatrix}\dot{V}\\ \dot{r}\end{bmatrix}=\begin{bmatrix}Y_V/M & Y_r/M-U\\ N_V/I_{zz} & N_r/I_{zz}\end{bmatrix}\begin{bmatrix}V\\ r\end{bmatrix}+\begin{bmatrix}0\\ 1/I_{zz}\end{bmatrix}\begin{bmatrix}T_{yaw}\end{bmatrix}+\begin{bmatrix}Y_\delta/M\\ N_\delta/I_{zz}\end{bmatrix}\begin{bmatrix}\delta\end{bmatrix} \quad (1)$$

or,

$$\dot{X}=AX+Bu+Gw$$

Where,

$$Y_V=\frac{-C_{\alpha f}-C_{\alpha r}}{U},\quad Y_r=\frac{-bC_{\alpha f}+cC_{\alpha r}}{U},\quad Y_\delta=C_{\alpha f}$$

$$N_V=\frac{-bC_{\alpha f}+cC_{\alpha r}}{U},\quad N_r=\frac{-b^2C_{\alpha f}-c^2C_{\alpha r}}{U},\quad N_\delta=bC_{\alpha f}$$

Where, M is the vehicle mass, I_{zz} is the mass moment of inertia around z-axis, $C_{\alpha f}$ is the front tire cornering stiffness, $C_{\alpha r}$ is the rear tire cornering stiffness, U is the longitudinal vehicle velocity, b is the distance from CG to front axle, c is the distance from CG to rear axle.

It is important to note that the YSC has access to both yaw rate and yaw acceleration. Hence, the final controller is a MISO (Multi Input Single Output) controller. The usual method of accessing yaw acceleration is to expand the state space with yaw acceleration by differentiating the state equations. However, an easier approach is to augment the output matrix C to obtain the yaw acceleration as follows,

$$\begin{bmatrix}r\\ \dot{r}\end{bmatrix}=\begin{bmatrix}0 & 1\\ N_V/I_{zz} & N_r/I_{zz}\end{bmatrix}\begin{bmatrix}V\\ r\end{bmatrix}+\begin{bmatrix}0\\ 1/I_{zz}\end{bmatrix}\begin{bmatrix}T_{yaw}\end{bmatrix}+\begin{bmatrix}0\\ N_\delta/I_{zz}\end{bmatrix}\begin{bmatrix}\delta\end{bmatrix} \quad (2)$$

or,

$$y=CX+D_2u+D_1w$$

The body yaw torque, T_{yaw} is then mapped statically to torque transfer (locking torque request).

The previous model contains the nominal plant P_0. The Hinf approach [8] requires augmentation of the nominal plant by shaping filters, as illustrated in Fig. 5, for derivation of the final controller.

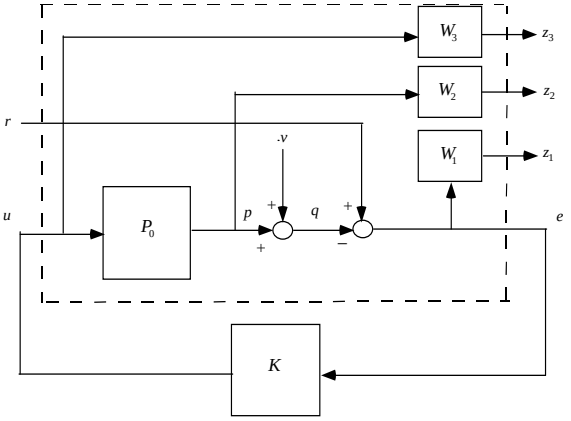

Fig. 5 Nominal augmented closed loop system

The filters that are used for the nominal plant augmentation are given as follows,

$$W_1=\begin{bmatrix}W_{11}=\dfrac{K\omega_n^2}{s^2+2\varsigma\omega_n s+\omega_n^2}\\ W_{12}=K\end{bmatrix} \quad (3)$$

Where, K is a constant, ω_n is the natural frequency and ς is the damping ratio. This filter matrix weights the sensitivity transfer function (disturbance input to controlled output). The W_{11} filter weights the sensitivity transfer function to the yaw rate output, while the W_{12} weights the sensitivity transfer function to the yaw acceleration output. It is also worth mentioning that the closed loop sensitivity transfer function follows the inverse of these filters. For example, the sensitivity transfer function to the yaw rate output, based on the shaping of the inverse of W_{11} filter, is small at low frequency and increases at high frequency. To simplify matters, the weighting for the yaw acceleration is used as a constant. Due to the limitation on the actuator bandwidth, the benefit of the yaw acceleration feedback is equivalently limited. As the actuator bandwidth is increased, the yaw acceleration feedback benefits become more apparent.

The shaping filter matrix, W_2, for the closed loop transfer function, (complementary transfer function), is given as follows,

$$W_2=\begin{bmatrix}W_{21}=\dfrac{K_1 s}{s+\dfrac{K_1}{T_{\max}}}\\ W_{22}=W_{21}\end{bmatrix} \quad (4)$$

This filter matrix is used as a weighting on the complementary transfer function so that that closed loop stability is guaranteed in the presence of the pure time delay of $T_{\max}$, due to the actuator dynamics.

A bode plot of a pure time delay of 0.1 second and the proposed weighting filter is illustrated in Figure

5.6. The constant K_1 and the weighting filter should be selected so that the weighting filter covers the entire frequency envelope of the pure delay, as illustrated in Fig. 6. At low frequency the weighting on the closed loop complementary transfer function is low and at higher frequencies this weighting increases, as the time delay effect becomes more severe. Hence, this weighting limits the bandwidth of the closed loop system with respect to the prescribed time delay.

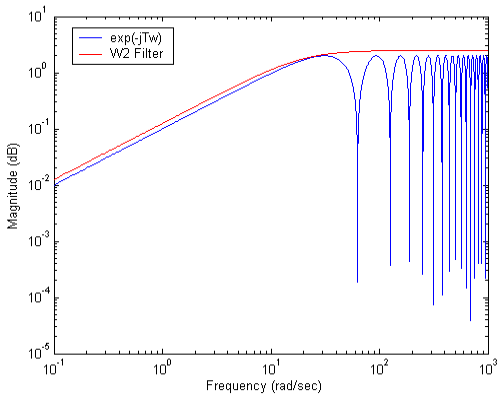

Fig. 6 Bode plot of W_2 filter (red) and pure time delay of 0.1 second (blue)

The final weighting filter is used to limit the actuator effort and is given by,

$$W_3 = \frac{1}{\rho} \tag{5}$$

Where, ρ is a constant and is equivalent to the maximum body yaw torque generated by the actuator. The feed-forward controller is derived by inverting the transfer function from the body yaw torque, T_{yaw}, to the yaw rate, r. Then, the steady state gain of this transfer function is used as a proportional gain for the feed-forward controller.

4. ON-VEHICLE RESULTS

The stability control performance of the system is analyzed in simulation and tested on-vehicle using several different maneuvers. The on-vehicle results of double lane change maneuver are presented in this section. Here the vehicle is driven through a defined double lane change course and the manoeuvre is carried out off throttle (the throttle is released at the entry gate) with the maximum initial speed that still allows the driver to steer through the cones without losing control of the vehicle. Due to the closed loop nature of this test, large numbers of both passive and controlled runs are required to ensure that the results are meaningful. In addition, passive and controlled runs are continuously interchanged to ensure comparable levels of tyre wear, tyre temperature, track condition and driver familiarity in each configuration. Also any runs where the initial speed significantly deviates from the target are discarded.

The steering wheel angle time histories for passive runs carried out with a target initial speed of 125kph are shown in Fig. 7. As can be observed, there is significant run to run variation and, in the majority of cases the driver is applying counter steer at some point in the maneuver.

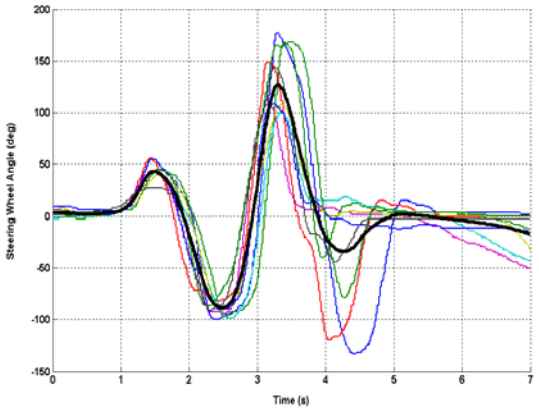

Fig. 7 Steering wheel angle time histories for 9 double lane changes carried out with a target initial speed of 125kph (average actual initial speed = 127.2kph). Passive vehicle. Average trace shown in black

This double lane change requires three distinct steering inputs, one to the left to steer towards the second gate, one to the right to steer through the second gate and towards the exit gate and one back to the left to return to straight ahead. Hence, if there is a fourth steering input (as there is in many of the runs), the vehicle is oversteering as it comes through the exit gate and the driver is applying counter steer. However, the vehicle can also begin to oversteer as it exits the second gate and hence the third steering input can also include counter steer. This point can be illustrated further by considering a specific example (Fig. 8). Here it is clear from the comparison of the reference and actual yaw rates (Fig. 8b) that the vehicle is oversteering after the second steering input as the two yaw rates have become significantly out of phase and the third steering input (Fig. 8a) is therefore (initially at least) counter steer, since the steering input and yaw rate are of opposite sign.

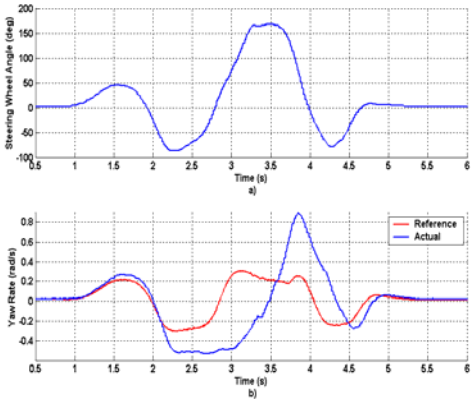

Fig. 8 Example of vehicle and driver behaviour during a passive double lane change carried out with a target initial speed of 125kph

The steering wheel angle time histories for 8 runs with the controller active are shown in Fig. 9. As can

be observed, there is significantly less run to run variation than in the passive case, which in itself is an indication that the vehicle is easier to drive. This increased consistency is illustrated by the dramatic reduction in the variance of the peak values of the third and fourth peak steering inputs of the controlled runs relative to the passive runs. Note that, in the controlled case, counter steer on the exit of the maneuver is largely eliminated (see below) so there is no fourth input.

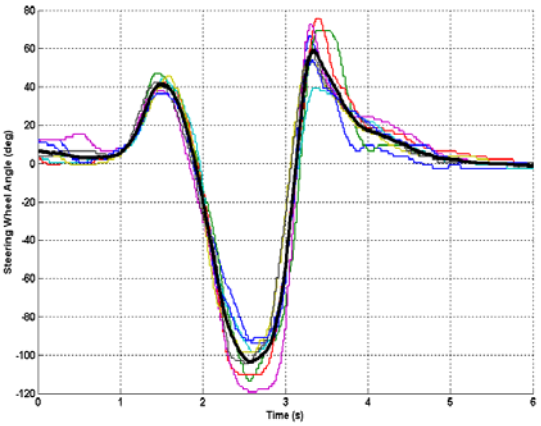

Fig. 9 Steering wheel angle time histories for 8 double lane changes carried out with a target initial speed of 125kph (average actual initial speed = 126.4kph). Active vehicle. Average trace shown in black

The impact of the ALSD on driver workload is shown clearly in Fig. 10 where the average steering inputs from the passive and active cases are compared. Here it can be observed that all counter steer on the exit of the maneuver has been eliminated and the magnitude of the third steering input has also been reduced by over 50%. In both cases this indicates significantly greater stability. Note that the validity of this conclusion is supported by the fact that there is less than 0.5% difference between the average actual entry speed for the two cases (127.2kph for passive and 126.4kph for controlled).

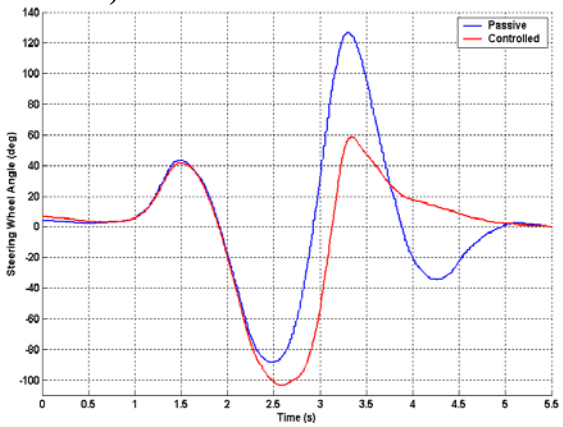

Fig. 10 Comparison of average steering wheel angle time histories for passive and controlled cases during a double lane changes carried out with a target initial speed of 125kph

Typical passive and controlled runs are compared in Fig. 11. Once again, it is clear from Fig.11a that driver workload is dramatically reduced. This is reflected in the controlled vehicle's yaw rate, which is now largely in phase with the reference yaw rate throughout the maneuver (Fig. 11b). This result confirms the observation made in the simulation environment that, even in an extreme maneuver such as this, the ALSD is still capable of forcing the vehicle to track the reference yaw rate, even if it does not do so precisely. It achieves this through the application of torque transfer from the point when the steering input begins to return to centre after going through the entry gate (Fig. 11c). The controller's request builds throughout the maneuver as the vehicle becomes more unstable with each successive steering input. However, because it is unable to force precise tracking of the reference yaw rate, the controller's request eventually reaches its saturation value. The ALSD runs out of authority here because, by 2.5 seconds, the differential has become locked, rendering further torque transfer impossible. This is reflected in Fig. 11c where it can be seen that the delivered torque transfer is no longer able to follow the requested torque transfer beyond this point (note the requested torque transfer is unsigned). This is therefore a confirmation of the effectiveness of an ALSD as a stability control device.

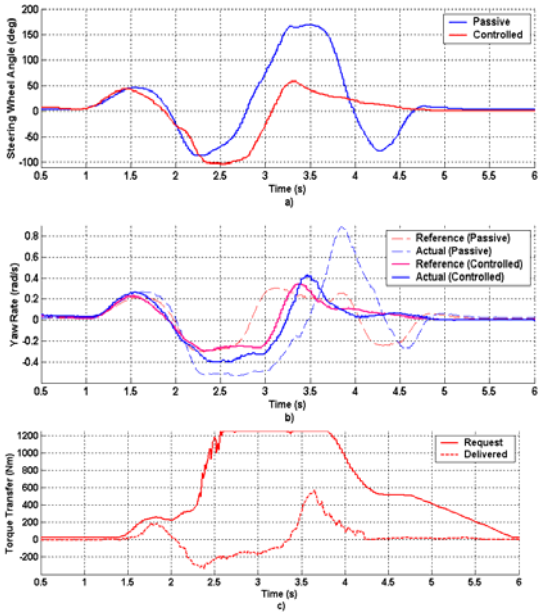

Fig.11 Comparison of passive and controlled example of driver, vehicle and controller behaviour during a double lane change carried out with a target initial speed of 125kph

5. CONCLUSION

In this paper, we have presented several different types of active differential and their potential use for increasing vehicle stability. Due to its hardware simplicity and lower cost, the ALSD is selected for further development. A MISO (Multi Inputs Single Output) robust Hinf controller is designed for the active control of the vehicle yaw. The effectiveness of the ALSD along with the Hinf controller is demonstrated on-vehicle through a double lane change manoeuvre. It

is important to note that although the Hinf controller is a linear controller, it is implemented on a highly non-linear actuator with a pure time delay of around 100ms and rise time of over 300ms. Furthermore, even though the ALSD is a semi-active device, only capable of transferring torque from a faster to a slower wheel, it has sufficient impact on the understeer gradient (yaw authority) to stabilize the vehicle under highly dynamic manoeuvres.

It is worthwhile stating that the ALSD is not designed to replace brake based stability controllers as it doesn't have nearly as much vehicle yaw authority as the brake based controllers. The synchronization of the ALSD and brake based stability controller has been investigated, although the results are not shown here; the two actuators complement each other extremely well. The ALSD is tuned to intervene much earlier than the brake based controller, so, when the brake based controller becomes active, it utilizes much lower brake pressures. This results in a very significant decrease of the actuator's intrusiveness. In addition, when the two actuators are working together, they have significantly more yaw authority and impact on the understeer gradient.

REFERENCES

[1] **Sawase, K., Sano, Y.,** 1999. "Application of Active Yaw Control to Vehicle Dynamics by Utilizing Driving/Braking Force", JSAE Review, **20**, pp. 289-295.

[2] **Hrovat, D., Asgari, J., Fodor, M.,** 2000. "Automotive Mechatronic Systems", Chap. 1 of "*Mechatronic Systems Techniques and Applications, Vol. 2: Transportation and Vehicular Systems*" (Leondes, C. T., ed.), CRC Press.

[3] **Deur, J., Hancock, M., Assadian, F.,** 2008, "Modeling and Analysis of Active Differential Kinematics", CD Proc. of 2008 ASME Dynamic Systems and Control Conference, Ann Arbor, MI.

[4] **Sawase, K., Ushiroda, Y., Miura, T.,** 2006, "Left-Right Torque Vectoring Technology as the Core of Super All Wheel Drive Control (S-AWC)", Mitsubishi Motors Technical Review, No. 18, pp.

[5] **Deur, J., Hancock, M., Assadian, F.,** 2008, "Modeling and of Active Differential Dynamics", DVD Proc. of IMECE2008, ASME Paper No. 2008-69248, Boston, MA.

[6] **Assadian, F., Hancock, M.,** 2005, "A Comparison of Yaw Stability Control Strategies for the Active Differential" Proc. Of 2005 IEEE International Symposium on Industrial Electronics, Dubrovnik, Croatia.

[7] **Hancock, M.J., Williams, R.A., Fina, E. and Best, M.C.**, 2007: Yaw motion control via active differentials, *Transactions of the Institute of Measurement and Control*, Vol 29, pp 137 – 157 16-23.

[8] **Mayne, D. Q.,** 1996, "Multivariable ControlSystem Design", unpublished course notes, Spring 1996.